

## Fast-switching phase gratings using in-plane addressed short-pitch polymer stabilized chiral nematic liquid crystals

Stephen M. Morris, Damian J. Gardiner, Flynn Castles, Philip J. W. Hands, Timothy D. Wilkinson et al.

Citation: *Appl. Phys. Lett.* **99**, 253502 (2011); doi: 10.1063/1.3670041

View online: <http://dx.doi.org/10.1063/1.3670041>

View Table of Contents: <http://apl.aip.org/resource/1/APPLAB/v99/i25>

Published by the [American Institute of Physics](#).

---

### Related Articles

A microsecond-response polymer-stabilized blue phase liquid crystal  
*Appl. Phys. Lett.* **99**, 201105 (2011)

Dielectric dispersion on the Kerr constant of blue phase liquid crystals  
*Appl. Phys. Lett.* **99**, 181126 (2011)

Phase diagram of the uniaxial and biaxial soft-core Gay-Berne model  
*J. Chem. Phys.* **135**, 134119 (2011)

Photo-aligned blend films of azobenzene-containing polyimides with and without side-chains for inducing inclined alignment of liquid crystal molecules  
*J. Appl. Phys.* **110**, 043522 (2011)

Opposite photo-induced deformations in azobenzene-containing polymers with different molecular architecture: Molecular dynamics study  
*J. Chem. Phys.* **135**, 044901 (2011)

---

### Additional information on *Appl. Phys. Lett.*

Journal Homepage: <http://apl.aip.org/>

Journal Information: [http://apl.aip.org/about/about\\_the\\_journal](http://apl.aip.org/about/about_the_journal)

Top downloads: [http://apl.aip.org/features/most\\_downloaded](http://apl.aip.org/features/most_downloaded)

Information for Authors: <http://apl.aip.org/authors>

### ADVERTISEMENT

**AIP**Advances

*Submit Now*

Explore AIP's new  
open-access journal

- Article-level metrics now available
- Join the conversation! Rate & comment on articles

## Fast-switching phase gratings using in-plane addressed short-pitch polymer stabilized chiral nematic liquid crystals

Stephen M. Morris, Damian J. Gardiner, Flynn Castles, Philip J. W. Hands, Timothy D. Wilkinson, and Harry J. Coles<sup>a)</sup>

*Centre of Molecular Materials for Photonics and Electronics, Electrical Engineering Division, Department of Engineering, University of Cambridge, 9 JJ Thomson Avenue, Cambridge CB3 0FA, United Kingdom*

(Received 10 October 2011; accepted 12 November 2011; published online 20 December 2011)

We demonstrate a fast-switching (sub-millisecond) phase grating based upon a polymer stabilized short-pitch chiral nematic liquid crystal that is electrically addressed using in-plane electric fields. The combination of the short-pitch and the polymer stabilization enables the diffraction pattern to be switched “on” and “off” reversibly in 600  $\mu\text{s}$ . Results are presented on the far-field diffraction pattern along with the intensity of the diffraction orders as a function of the applied electric field and the response times. © 2011 American Institute of Physics. [doi:10.1063/1.3670041]

Liquid crystals (LCs) have shown considerable promise as electrically addressable phase gratings.<sup>1–4</sup> Most LC phase gratings reported in the literature are based upon nematic technology that are subjected to different electric field configurations or patterns that lead to the diffracting element. Research has also been conducted on chiral nematic LCs where diffraction can arise from refractive index variation due to a modulated “finger print” texture.<sup>5,6</sup> In general, the main limitation with these collective technologies is the time required for the LC to respond, which is typically of the order of 10–100 ms.

There are alternative LC electro-optic effects that exhibit much more rapid rise and decay response times. One example is blue phase (BP) LCs, which has attracted renewed interest due to the development of wide temperature range materials that occur either naturally<sup>7,8</sup> or through the use of polymer stabilization.<sup>9</sup> Recently, phase gratings based upon these materials have been reported, which have a much shorter response time than conventional nematic gratings.<sup>10</sup> However, at present, these devices require special processing conditions to create the structure such as photo-polymerization at a precise temperature.

In this letter, we demonstrate that short-pitch polymer stabilized chiral nematics can be used to form phase gratings that respond in equally rapid rise and decay times to that observed for blue phase devices. This is based upon a mode of operation consisting of very short pitch chiral nematic LCs (<250 nm) that are electrically addressed with in-plane switching (IPS) technology when in the uniform standing helix (USH) geometry.<sup>11,12</sup> An illustration of the device configuration and the change in the optical indicatrix with an applied electric field between the in-plane electrodes is shown in Fig. 1.

The chiral nematic mixture was based upon a commercially available nematic LC (MDA-00-3506, Merck KGaA) that was doped with a relatively low concentration (7 wt. %) of the high twisting power chiral dopant (R5011, Merck KGaA) so as to form a chiral nematic with a pitch that was

less than 250 nm. To this mixture was added a reactive mesogen (RM257, concentration = 7 wt. %) and photo-initiator (Irgacure 819, concentration = 0.7 wt. %) that would later form the polymer network. Cells consisted of one substrate that had been coated with an inter-digitated indium-tin-oxide structure (150 nm-thick) that provided the lateral (in-plane) electric field (fabricated by LG Display). The separation between successive electrodes was  $s = 9 \mu\text{m}$  (inter-electrode spacing) and each had a width of  $w = 4 \mu\text{m}$ .  $5 \mu\text{m}$  spacer beads were used to set the cell gap. After capillary filling the mixture into the cell, exposure (15 min duration) with ultraviolet light at a wavelength of 365 nm and a power density of  $5 \text{ mW}/\text{cm}^2$  resulted in the formation of a polymer network that stabilized the chiral nematic structure.

Insight into the phase profile of the device may be gained from a polarizing optical microscope image of the polymer stabilized chiral nematic when subjected to an electric field of  $14 \text{ V}/\mu\text{m}$ , Fig. 2. These images were recorded at a temperature of  $25^\circ\text{C}$  on a high magnification polarizing microscope (BX60, Olympus) using crossed polarizers. In the absence of an electric field, the cell appears dark between crossed polarizers because, at normal incidence, there is no net retardation and the sample appears uniformly optically inactive (cf. Fig. 1(b)). With the application of an electric field with a frequency of 1 kHz, an effective birefringence is induced in the plane of the device between the electrode pixels, which increases as the strength of the field is increased. In this region, the intensity of the light that is transmitted increases with the electric field, whereas the regions directly above the electrodes remain dark. As a result, the intensity profile across the cell, which is shown in the graph at the top of Fig. 2, is approximately a two-level step function.

A linearly polarized He-Ne laser ( $\lambda = 632.8 \text{ nm}$ ) was used to generate a diffraction pattern in the far-field at a distance of 25 cm from the sample. Figure 3 is a collection of photographs of the resulting diffraction pattern for four different electric field strengths when the plane of polarization was along the same direction as the applied electric field. In the absence of an electric field, only a single zeroth order spot is observed. As the field strength  $E$  is increased to approximately  $7 \text{ V}/\mu\text{m}$ , the  $\pm 1$  orders ( $\theta = 3.1^\circ$ ) become

<sup>a)</sup> Author to whom correspondence should be addressed. Electronic mail: hjc37@cam.ac.uk.

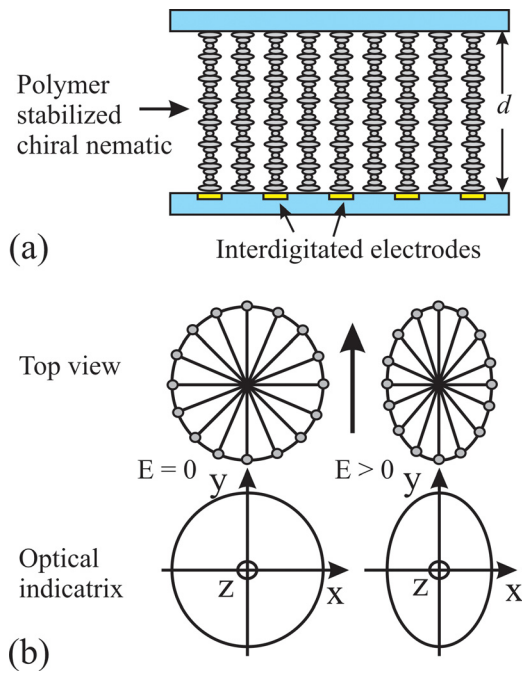


FIG. 1. (Color online) Illustration of (a) the device configuration and (b) the change of the optical indicatrix with an applied electric field.

visible, whereas the  $\pm 2$  orders ( $\theta = 6.1^\circ$ ) are only just beginning to appear.

Here  $E$  is calculated as the applied voltage at the electrodes divided by the electrode separation,  $s$ , and no attempt has been made to correct for the reduced electric field in the inter-electrode volume due to the surface electrodes. Following Kim *et al.*, one might expect the effective internal field to be reduced by approximately a factor of 3.<sup>13</sup> The intensity contained with each order continues to increase as the field strength increases and eventually the  $\pm 3$  orders ( $\theta = 9.1^\circ$ ) become visible at around  $14 \text{ V}/\mu\text{m}$ . Since these measurements were carried out at normal incidence, we can apply the standard relationship of  $\Lambda \sin \theta = m\lambda$  to determine the grating period,  $\Lambda$ , which is found to be  $12 \pm 1 \mu\text{m}$ . This is in good agreement with the dimensions of the inter-electrode spacing and the electrode width ( $\Lambda = s + w = 13 \mu\text{m}$ ). The

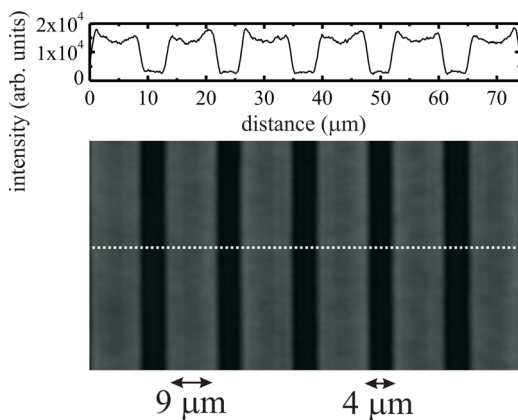


FIG. 2. (Color online) Photograph of the short pitch polymer-stabilized chiral nematic liquid crystal between crossed polarizers for an electric field strength of  $E = 14 \text{ V}/\mu\text{m}$  with a bipolar square wave at a frequency of 1 kHz. The grating period is  $\Lambda = 13 \mu\text{m}$ . A plot of the intensity profile is also shown.

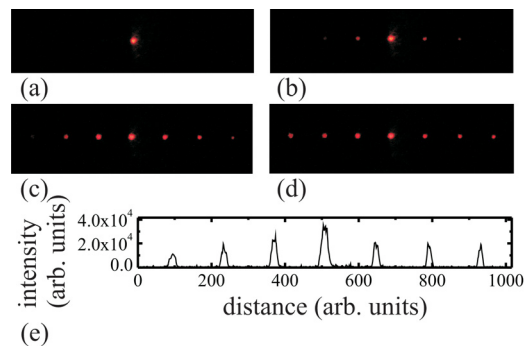


FIG. 3. (Color online) Photographs of the far-field diffraction pattern for different electric field strengths of a bipolar square wave with a frequency of 1 kHz. (a)  $E = 0 \text{ V}/\mu\text{m}$ , (b)  $E = 7 \text{ V}/\mu\text{m}$ , (c)  $E = 14 \text{ V}/\mu\text{m}$ , and (d)  $E = 29 \text{ V}/\mu\text{m}$ . (e) The intensity profile of the diffraction pattern for  $E = 29 \text{ V}/\mu\text{m}$ . The incident laser wavelength was  $\lambda = 632.8 \text{ nm}$  and the results are for an input polarization that is parallel to the E-field direction.

graph shown in Fig. 3(e) represents the intensity profile across the diffraction pattern and it is clear that the 1st, 2nd, and 3rd orders are present. In this case, the 2nd order is not suppressed due to the mismatch in the dimensions between the inter-electrode region and the electrode region.

The relative intensity of the zeroth order as well as the  $+1$  and  $+2$  orders are plotted in Fig. 4 as a function of the applied electric field strength at a temperature of  $25^\circ\text{C}$ . For each data set, the intensity was recorded in the far-field at a distance of 25 cm from the sample by a fast photodiode that was connected to a digitizing oscilloscope (Agilent). A Glan-Taylor polarizer was used to define the input polarization at the sample, and an iris placed before the detector ensured that only the intensity of one order was recorded at any one time. As the electric field strength is increased, the intensity in the zeroth order is decreased as energy is transferred to the higher orders. Maximum diffraction efficiency is achieved at an electric field strength of  $23 \text{ V}/\mu\text{m}$ . At normal incidence, identical curves are obtained for the  $-1$  and  $-2$  orders. The diffraction efficiency, defined as the intensity of the  $+1$ st order relative to the total intensity of the zeroth order in the absence of an applied electric field, is found to be  $\approx 20\%$ . This is comparable to conventional nematic and non-polymer stabilized chiral nematic devices but somewhat lower than that observed recently for BPLC phase gratings.

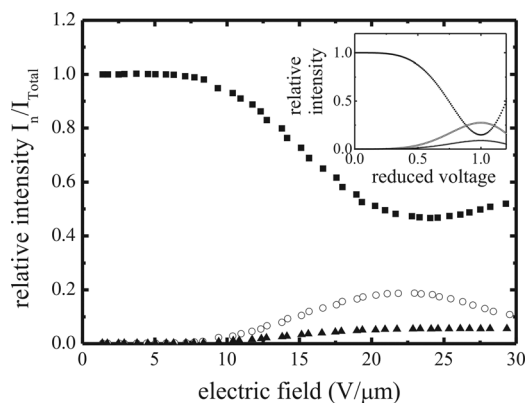


FIG. 4. A plot of the ratio  $I_n/I_{\text{Total}}$  (the intensity of the  $n$ th diffraction order/the total intensity of the zeroth order for  $E = 0 \text{ V}/\mu\text{m}$ ) as a function of the electric field strength. Three orders are shown: zeroth (squares),  $+1$ st (circles), and  $+2$ nd (triangles). The inset corresponds to the theoretical results obtained using the expressions provided in Eqs. (1) and (2).

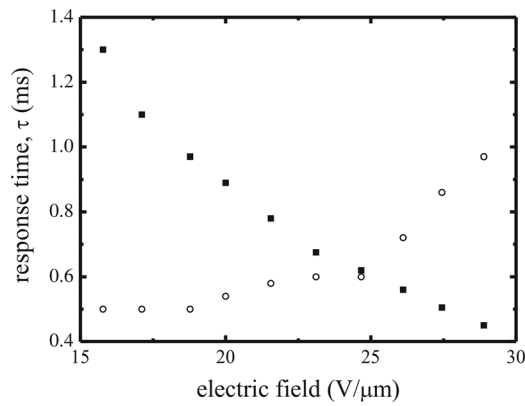


FIG. 5. Response times of the diffraction grating to an isolated bipolar pulse train as a function of the electric field strength. Rise times (squares) and fall times (circles).

The qualitative behaviour of the device can be accounted for using a simple analytic model. Using the intensity profile plot shown in Fig. 2 as an indication of the phase profile across the device, the far field diffraction pattern can be calculated from the Fourier transform of the approximate two-level aperture function:  $f = \exp(i\theta)$  between the electrodes and  $f = 1$  above the electrodes. The relative phase  $\theta$  is proportional to the square of the applied voltage  $\theta = \alpha V^2$ . This gives the normalized zeroth order transmitted intensity as a function of applied voltage

$$I_0 = 1 + 2 \frac{s}{\Lambda} \left( \frac{s}{\Lambda} - 1 \right) (1 - \cos(\alpha V^2)) \quad \text{for } n=0 \quad (1)$$

and the  $n$ th order transmitted intensity

$$I_n = \frac{2}{n^2 \pi^2} \sin^2 \left( n\pi \frac{s}{\Lambda} \right) (1 - \cos(\alpha V^2)) \quad \text{for } n = \pm 1, \pm 2, \pm 3, \dots \quad (2)$$

The curves are shown in the inset of Fig. 4(a) where it can be seen that there is a good qualitative agreement with the experimental data ( $s = 9 \mu\text{m}$  and  $\Lambda = 13 \mu\text{m}$ ). To achieve quantitative agreement, it would seem necessary to describe the phase profile more accurately. The analytic model shows that the diffraction efficiency may be expected to increase if the inter-electrode spacing is equal to the electrode width ( $s = \Lambda/2$ ). This may explain the lower diffraction efficiency of our device with respect to the BPLC grating of Ref. 10 for which the  $s = \Lambda/2$  condition was realized.

The chiral nematic phase gratings are found to be polarization dependent. Results showed that the phase modulation is greatest for the polarization parallel to the applied electric field although there is a weak modulation for the orthogonal polarization. This corresponds with the greater contrast in the effective refractive indices in the direction of the applied

electric field. Due to the complexity of the structure, an exact description of the director profile is not yet known when the electric field is applied but this does not affect our treatment in the present study.

Evidence of the short response times of the phase grating is presented in Fig. 5. Here the rise and decay times represent the time required for the intensity of the zeroth order to respond to a train of bipolar pulses at a frequency of 1 kHz. The rise and decay times correspond to a 10%–90% and 90%–10% change in the transmission level, respectively. These times have different dependencies upon the electric field strength but at values corresponding to maximum diffraction efficiencies ( $E = 23 \text{ V}/\mu\text{m}$ ) both the rise and decay times are substantially below 1 ms being  $\tau \approx 600 \mu\text{s}$ . It is important to note that a significant reduction of the response time can be achieved by further decreasing the pitch of the helix or by operating at slightly elevated temperatures (e.g.,  $35^\circ\text{C}$ ).<sup>11</sup>

In summary, we have presented a phase grating based upon a short-pitch polymer stabilized chiral nematic LC. By virtue of the short pitch, the time required for the diffraction pattern to be generated is  $\approx 600 \mu\text{s}$ . Furthermore, by polymer stabilizing the structure, the generation and removal of the diffraction pattern is fully reversible. Further improvements to the material and the device architecture will enable lower voltages and higher diffraction efficiencies to be realised making these LC phase gratings promising for applications which demand sub-millisecond timescales.

This work was carried out under the COSMOS project (EP/H046658/1) which is funded by the Engineering and Physical Sciences Research Council (UK). One of the authors (SMM) acknowledges The Royal Society for funding.

<sup>1</sup>R. G. Lindquist, J. H. Kulick, G. P. Nordin, J. M. Jarem, S. T. Kowel, M. Friends, and T. M. Leslie, *Opt. Lett.* **19**, 670 (1994).

<sup>2</sup>J. H. Kulick, J. M. Jarem, R. G. Lindquist, S. T. Kowel, M. W. Friends, and T. M. Leslie, *Appl. Opt.* **34**, 1901 (1995).

<sup>3</sup>I. Fujieda, *Appl. Opt.* **40**, 6253 (2001).

<sup>4</sup>L. Gu, X. Chen, W. Jiang, B. Howley, and R. T. Chen, *Appl. Phys. Lett.* **87**, 201106 (2005).

<sup>5</sup>D. Subacius, P. J. Bos, and O. D. Lavrentovich, *Appl. Phys. Lett.* **71**, 1350 (1997).

<sup>6</sup>D. Subacius, S. V. Shiyonovskii, Ph. Bos, and O. D. Lavrentovich, *Appl. Phys. Lett.* **71**, 3323 (1997).

<sup>7</sup>H. J. Coles and M. N. Pivnenko, *Nature* **436**, 997 (2005).

<sup>8</sup>F. Castles, S. M. Morris, and H. J. Coles, *Phys. Rev. Lett.* **104**, 157801 (2010).

<sup>9</sup>H. Kikuchi, M. Yokota, Y. Hiskado, H. Yang, and T. Kajiyama, *Nature Mater.* **1**, 64 (2002).

<sup>10</sup>J. Yan, Y. Li, and S.-T. Wu, *Opt. Lett.* **36**, 1404 (2011).

<sup>11</sup>D. J. Gardiner, S. M. Morris, F. Castles, M. M. Qasim, W.-S. Kim, S. S. Choi, H.-J. Park, I.-J. Chung, and H. J. Coles, *Appl. Phys. Lett.* **98**, 263508 (2011).

<sup>12</sup>F. Castles, S. M. Morris, and H. J. Coles, *Phys. Rev. E* **80**, 031709 (2009).

<sup>13</sup>M. Kim, M. S. Kim, B. G. Kang, M.-K. Kim, S. Yoon, S. H. Lee, Z. Ge, L. Rao, S. Gauza, and S.-T. Wu, *J. Phys. D: Appl. Phys.* **42**, 235502 (2009).